Available online at www.sciencedirect.com
ScienceDirect
Separation and Purification Technology 58 (2007) 192–199
Separation Purification Technology
www.elsevier.com/locate/seppur

Preparation of highly ordered titanium dioxide porous films: Characterization and photocatalytic activity

Ruey-an Doong [a,*], Sue-min Chang [b], Yu-chin Hung [a], I-ling Kao [a]

[a] *101, Sec. 2, Kuang Fu Road, Department of Biomedical Engineering and Environmental Sciences, National Tsing Hua University, Hsinchu 30013, Taiwan*
[b] *75, Po Ai Street, Graduate Institute of Environmental Engineering, National Chiao Tung University, Hsinchu 30068, Taiwan*

Abstract

The highly ordered titanium dioxide (TiO_2) porous films was fabricated by a single-step assembly method in which the fabrication of opal structure and the infiltration of TiO_2 sol particles into the voids between templates were carried out simultaneously. The polystyrene microspheres with diameters ranging between 480 and 1000 nm were used as the template, and titanium tetrabutoxide, a precursor of TiO_2, was prepared in an acidic solution to fill the voids between the template microspheres during the formation of opal structure. The properties of the highly ordered TiO_2 porous materials were examined by scanning electron microscopy (SEM), thermogravimetry (TA), differential scanning calorimetry (DSC), X-ray diffraction (XRD) and specific surface area analyzer. Thermal analyses showed that polystyrene can be completely removed at 425 °C and the phase transformation of TiO_2 from amorphous to crystalline anatase occurred at 360 °C. SEM images clearly demonstrated that these films have a highly ordered three-dimensional porous structure arranged mainly in hexagonal orientation. The XRD patterns indicated that the crystalline phase of TiO_2 is mainly anatase with crystallite sizes of 7.0–9.7 nm. In addition, the ratio of rutile to anatase increased slightly with the increase in hole diameters of the ordered TiO_2 porous films. The specific surface areas of the ordered TiO_2 porous film ranged between 59 and 84 $m^2\ g^{-1}$, and the determined adsorption pore sizes in walls between templates were in the range 5.1–6.0 nm, which indicates that the fabricated TiO_2 film is a macrostructured mesoporous material. The ordered TiO_2 porous films showed high photocatalytic activity in degradation of methylene blue (MB) solution. The degradation rate increased linearly with the increase in hole diameters of the TiO_2 films ranging between 480 and 1000 nm. Results obtained in this study clearly show the feasibility of using one-step method to fabricate the highly ordered TiO_2 materials as potential supports for heterogeneous catalysis.

Keywords: Ordered TiO_2 porous films; Sol–gel; Template; Photocatalytic activity

1. Introduction

The fabrication of porous nanocrystalline titanium dioxide (TiO_2) has recently attracted much attention in terms of their versatile applications in solar cell, electrical and photocatalytic systems because it is highly stable, non-toxic, and has a suitable redox potential for photodegrading pollutants [1–3]. Several studies have focused on the use of TiO_2 nanoparticle for the purpose of improving the photocatalytic efficiency with respect to the high surface-to-volume ratio [4–7]. However, the disadvantages of TiO_2 particles, such as easy loss of photocatalytic activity, agglomeration and difficulty in being recovered, hamper its application to photocatalytic systems. Several studies immobilized TiO_2 onto the surfaces of carriers to overcome these drawbacks and such materials have been used repeatedly [8–10]. However, the immobilization process of nanocrystalline TiO_2 usually lowered the surface area and increased the band gap of TiO_2, resulting in the decrease in photocatalytic efficiency and rate. Therefore, the development of the immobilization technique that can maintain high surface area and excellent physicochemical properties of TiO_2 for photocatalysis is thus required.

Highly ordered three-dimensional porous TiO_2 structure with lattice spacing on the order of wavelengths of light is one of the promising materials that can be used as photocatalyst in visible light region [11–13]. Usually, the fabrication of hierarchical porous materials involves two steps: to form a highly ordered opal structure first and then to infiltrate materials into the voids in the opal structure to solidify the porous structure. The first step for arranging a highly qualified opal structure is the critical

* Corresponding author. Tel.: +886 3 5726785; fax: +886 3 5718649.
E-mail address: radoong@mx.nthu.edu.tw (R.-a. Doong).

1383-5866/$ – see front matter © 2007 Elsevier B.V. All rights reserved.
doi:10.1016/j.seppur.2007.07.029

step for fabricating a perfectly ordered porous structure. Of the various methods used for fabricating ordered porous films, the template method is the most often used technique because the dimensions of the pores are set by the size of the ordered template beads and the pore size can be varied easily [11–19]. Several templates including SiO_2, polystyrene, poly(methyl methacrylate), and surfactant have been employed to create macroporous TiO_2 structure [11–16]. After the formation of opal structures, nanoparticles such as inorganic oxides, alloys, sol–gel-derived metal oxides, metal particles, carbons, and polymers can be infiltrated between voids of templates by chemical vapor deposition (CVD), filtration, vertical dipping, or electrochemical technique to form highly ordered porous material [17–22].

It is well accepted that the preparation of a high-quality opal structure and the complete infiltration of the voids of the template without damage of the template itself when filled are the major factors influencing the quality of the porous structure fabricated by the two-step method. However, the infiltration processes usually impede the opal structure because of the difficulty in controlling the driving force of infiltration such as vacuum, negative pressure, and capillary force [23,24]. In addition, the filler cannot be infiltrated well because the fillers have to move a long distance during the infiltration process. Therefore, the development of one-step methods that incorporate the formation of opal structure with the infiltration of filler at the time is of urgent needed. Meng et al. [25] have recently developed a cooperative assembly method which could simply fabricate the highly ordered TiO_2 films by infilling commercial ultra-fine particles into the voids of the templates. However, the size of the ultra-fine particles used for infiltration is unlikely to be easily changed. Sol–gel method is a size-tailored technique and has been widely used for the preparation of nanocrystalline particles including TiO_2, SiO_2 and ZrO_2 [26–29]. The combination of template and sol–gel methods has the advantages of simple preparation and size-tailoring, and homogeneity of sol–gel products with high isotropy of physical, morphological and chemical properties, thus allowing the fabrication of highly ordered porous materials in a single-step. In addition, the photocatalytic activity of the ordered TiO_2 porous films has received less attention.

In this study, a single-step method incorporating the sol–gel and template methods using titanium dioxide (TiO_2) sol and polystyrene as the filler and template, respectively, was developed to fabricate an ordered TiO_2 porous film. Scanning electron microscopy (SEM) and X-ray diffraction (XRD) were used to examine the surface morphologies and the crystallization properties of the ordered TiO_2 porous structures. The thermal analysis using thermogravimetry-differential scanning calorimeter (TG-DSC) was also employed to understand the thermal properties of solvent and polystyrene particles. In addition, the UV–vis spectrophotometer and surface analyzer were also used to examine the optical properties and specific surface areas of the hierarchical TiO_2 porous materials. Methylene blue (MB) was selected as the model compound to examine the photocatalytic activity of the ordered TiO_2 porous films. The activity of the novel TiO_2 photocatalyst was compared with that of Degussa P-25.

2. Experimental

2.1. Chemicals

All chemicals were used as received without further treatment. Titanium tetrabutoxide (99%) and cetyltrimethylammonium chloride (CTAC) were purchased from Alfa Aesar Co. (Ward Hill, MA). Anhydrous ethanol was purchased from Fluka (Buchs, Switzerland). Monodispersed polystyrene with diameters of 480, 600, and 1000 nm were purchased from Duke Scientific Corporation (Palo Alto, CA). All the solutions were prepared with high-purity bidistilled deionized water (Millipore, 18.3 $M\Omega\,cm^{-1}$).

2.2. Preparation of ordered porous films

The sol solution of titanium dioxide was prepared by dissolving 0.1 mL of titanium tetrabutoxide in 0.9 mL of anhydrous ethanol in a sealed polyethylene tube. Then, 9 mL of hydrochloric acid solution was added into the polyethylene tube. The latex solutions of the polystyrene template with diameters ranging between 480 and 1000 nm were prepared at concentration of 0.2% by diluting the polystyrene latex solution with deionized water, and then dispersing the polystyrene particles ultrasonically in the solution.

The ordered TiO_2 porous films were fabricated using capillary forces to drive the polystyrene and TiO_2 sol particles to assemble at the same time. The glass substrates (2.5 cm × 7.5 cm) were first cleaned using $K_2Cr_2O_7/H_2SO_4$ solution that was prepared by 0.84 g of $K_2Cr_2O_7$, 7 mL of deionized water and 200 mL of concentrated sulfuric acid in order to remove any organic contaminant on the substrate. The substrates were immersed in the chromic–sulfuric acid solution overnight, rinsed with the copious deionized water thoroughly, and then dried under a stream of nitrogen. After full dispersion of polystyrene latex, TiO_2 sol particles, and 10 μL CTAC by ultra-sonication in a 15-mL silanized glass vial, the hydrophilic glass substrate was vertically immersed into the glass vial. This fabricated system was placed on a hot plate at 55 °C and the relative humidity was controlled at 40–60%. The opal structures of polystyrene can be formed by capillary forces during the evaporation of water and solvent molecules at 55 °C. After the formation of opal structures, the glass substrate in the glass vial was then taken out and placed on a heating apparatus at 80 °C for 30 min to enhance the structural strength. Finally, the opal structures were calcined at 550 °C for 2 h to obtain an ordered TiO_2 porous material.

2.3. Characterization

The surface morphology of the ordered TiO_2 porous film was determined by SEM (Hitachi S-4700 type II, Tokyo, Japan). All the samples were Pt-coated using Ion Sputter ε-1030 (Hitachi, Japan) to increase the conductivity of the sample surface. After coating with Pt, samples were placed under high vacuum (10^{-3} to 10^{-7} mbar) condition. An acceleration electron voltage of 5 kV voltage was applied to obtain the SEM images.

The crystalline properties of the TiO_2 films were analyzed by an X-ray diffractometer (XRD, Philips X'Pert Pro) using Cu Kα radiation (λ = 1.5406 Å) and operating at an accelerating voltage of 45 kV and an emission current of 40 mA. A grazing angle mode was applied at an incident angle of 1°. Data were acquired over the range of 2θ from 10 to 90° at a sampling width of 0.02° and a scanning speed of 4° min^{-1}.

The thermal properties of TiO_2 porous films were performed using a TG-DSC thermal analyzer (Setaram Labsys, Caluire, France). The temperature increased from room temperature to 600 °C at a rate of 2.5 °C min^{-1} under ambient conditions and the flow rate of air was 30 mL min^{-1}. The specific surface area and pore size distribution studies were determined by nitrogen adsorption isotherms measured at 77 K using a N_2 adsorption analyzer (Micromeritics ASAP 2020). The Brunauer, Emmett and Teller (BET) and Barrett, Joyner and Halenda (BJH) models were used to estimate the surface area and pore volume of the TiO_2 films according to the nitrogen adsorption isotherms.

The optical property was measured using a UV–vis spectrophotometer equipped with a HITACHI S-3010 controller UV solution (Hitachi 1.4, Tokyo, Japan). The scanning wavelength range is from 200 to 800 nm at a scan rate of 60 nm min^{-1}. In the UV–vis spectroscopy, a spectrophotometer was used by passing a single wavelength beam of light through a sample with a fixed optical path length. The spectrophotometer monitors the absorption of light by the sample. In the wavelength-scanning mode, the wavelength of the incident light varied over time to allow the spectrophotometer to create a characteristic spectrum.

2.4. Photocatalyic activity of ordered porous films

Methylene blue (MB) was selected as the target compound to examine the photocatalytic activity of the fabricated ordered TiO_2 porous films. The photocatalysts were suspended in the MB solutions (10 μM) to get a dosage of 0.3 g/L in the dark. Photocatalytic reactions were carried out in a quartz tube irradiated by UV light at the wavelength of 305 nm. The suspensions were withdrawn at intervals and filtrated using 0.45 μm filters to remove solids. The residual concentrations of MB in supernatants were then determined at 664 nm using UV–vis spectrophotometer.

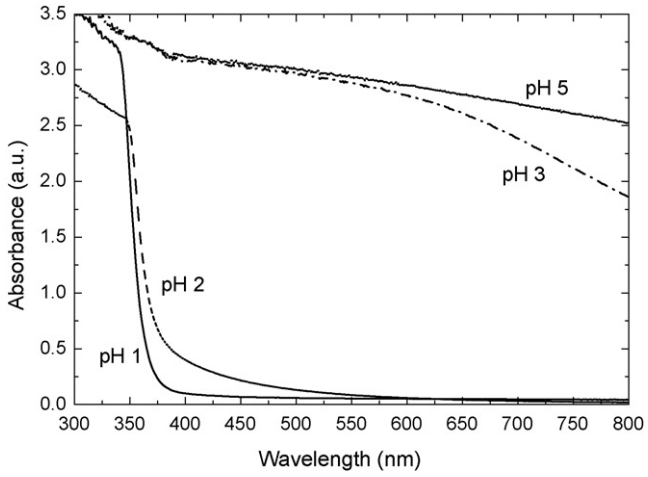

Fig. 1. The UV–vis spectra of TiO_2 sol solution at pH values ranging between 1.0 and 5.0.

3. Results and discussion

3.1. Effect of pH on titania sol

The sol–gel is a pH sensitive process and the pH value of the sol solution is a crucial parameter controlling the particle size of TiO_2, which may influence the fabrication of a highly ordered porous structure using a dipping method. In this study, different pH values of HCl solution ranging between 1 and 5 were examined in the sol–gel process to understand the formation characteristics of TiO_2. Fig. 1 shows the UV–vis spectra of TiO_2 sol solution prepared at various pH values. The sol solution at pH 1.0 appeared to be slurry initially, and became transparent when stood overnight. In the pH range of 1.0–5.0, the gelation rate of TiO_2 sol was fast, and white solid precipitates were formed immediately when HCl solution was added. The absorption of TiO_2 solution shifts to a long wavelength when pH increased from 1 to 5, indicating that the size of sol particle increased with increasing pH values. Fig. 2 shows the TEM images of TiO_2 sol particles at pH values of 1.0 and 2.0. The grain size of TiO_2 sol at pH 1.0 was about 5.3 ± 2.2 nm ($n = 20$), and aggregated to a bigger particle size in solution. The TiO_2 sol particles increased dramatically to 20 ± 5.6 nm ($n = 20$) when acid solution at pH 2.0 was added, clearly depicting that the HCl solution at pH

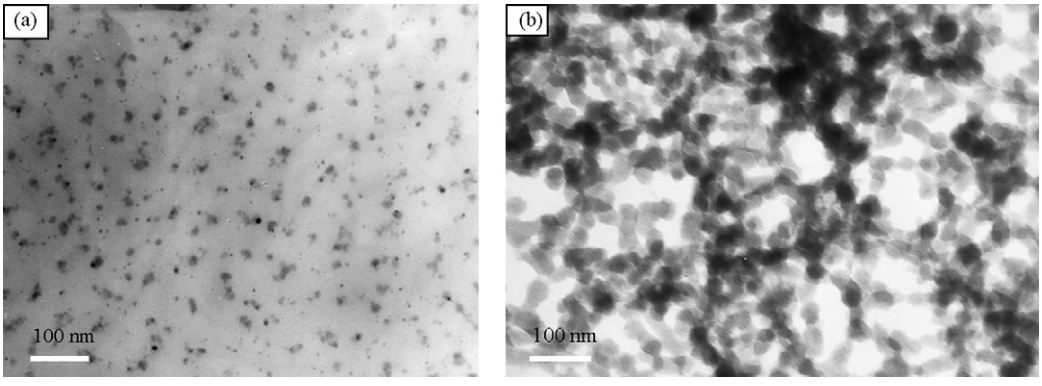

Fig. 2. The TEM images of TiO_2 sol solutions at pH values of (a) 1.0 and (b) 2.0.

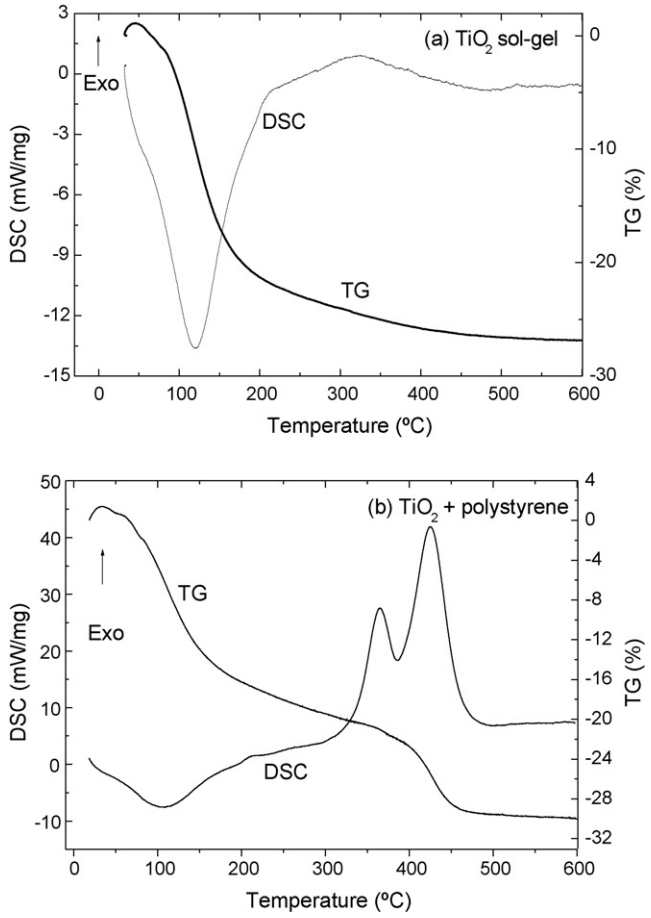

Fig. 3. Thermal analysis of (a) TiO_2 sol–gel and (b) titania-polystyrene composites after heat treatment from room temperature to 600 °C.

1.0 is the optimal solution for sol–gel process to produce small particles of TiO_2 for infiltrating the voids of the opal structure.

3.2. Thermal analysis of ordered porous materials

To understand the thermal properties of the fabricated porous TiO_2 film, TG and DSC were employed to determine the change in weight loss and entropy, respectively. The temperature increased from room temperature to 600 °C at a rate of 2.5 °C min^{-1} under ambient conditions and the flow rate of air was 30 mL min^{-1}. Fig. 3 shows the TG and DSC curves of pure sol–gel-derived TiO_2 and the mixture of titania sol–gel and 600 nm polystyrene. In the pure TiO_2 sol–gel film, the endothermic and exothermic peaks are clearly observed on the DSC curve. A broad endothermic peak occurring at 105 °C with weight loss of 26% indicates the evaporation of HCl and water from the TiO_2 sol–gel matrix. In addition, an exothermic peak appeared at 320 °C with little weight loss, presumably attributed to the removal of the crystal water in internal titanium dioxide and the phase transformation from amorphous to crystalline TiO_2.

The thermal properties of the opal structure fabricated with TiO_2 and 600 nm polystyrene were further determined. As depicted in Fig. 3b, an endothermic peak with a weight loss of 17% was clearly observed at 108 °C, which is similar to the results obtained in the pure TiO_2 sol–gel film. In addition, two exothermic peaks were observed. The first exothermic peak at 360 °C with little weight loss is attributed to the phase transformation from amorphous structure to crystalline TiO_2, which is in good agreement with the previous study [15]. Another exothermic peak appeared at 425 °C, presumably due to the decomposition of polystyrene and surfactant. The TG curve showed a decrease in mass of about 6.5%. Several studies showed that the phase transformation of anatase to rutile started in the temperature range of 400–600 °C [15,30,31]. Yu et al. [15] reported that the optimal calcinations temperature for mesoporous TiO_2 thin films prepared with surface-templated sol–gel method was 500 °C, at which the film exhibited the highest photocatalytic activity. In this study, the calcination temperature of 550 °C was selected for the fabrication of ordered porous titanium dioxide in order to completely decompose the organics and transform amorphous TiO_2 into the crystal phase.

3.3. Fabrication of ordered TiO_2 porous films

With the evaporation of liquid fluxes through the voids of the template and capillary forces to assemble themselves, the TiO_2 colloids can infill the voids of the template as a result of a convective water flux that carries the colloid toward the voids. Therefore, it is important to optimize the concentration of the mixture of TiO_2 sol and polystyrene solution for the fabrication of a highly ordered porous structure. Table 1 shows the optimal conditions for fabricating highly ordered porous structures using polystyrene of different sizes. When 480 and 600 nm polystyrene were used as the templates, highly ordered porous titanium dioxide structures can be obtained when the volumes of TiO_2 sol, polystyrene solution (0.2%), and CTAC were 0.4, 0.5 mL, and 10 μL, respectively. However, the use of 1000 nm polystyrene as the template could not obtain an ordered porous structure under the same conditions, presumably due to the different convection flow fluxes and capillary forces when different particle sizes of polystyrene were used. After increasing the polystyrene solution to 1.0 mL, an ordered porous structure could then be obtained.

Fig. 4 shows the SEM images of ordered TiO_2 porous structures at different magnifications on glass substrates after calcination at 550 °C. The porous structures were prepared using polystyrene microspheres with diameters of 480, 600, and 1000 nm. These images show a typical area on the surface with multiple domains of nanocrystalline pores that have the

Table 1
Optimization of sol–gel processes for the fabrication of opal structures using different particle sizes of polystyrene as templates

Polystyrene size (nm)	1% TiO_2 sol (mL)	0.2% PS solution (mL)	D.I. water (mL)
480	0.4	0.5	1.1
600	0.4	0.5	1.1
1000	0.4	1.0	0.6

The preparation temperature and relative humidity were 55 °C and 40–60%, respectively.

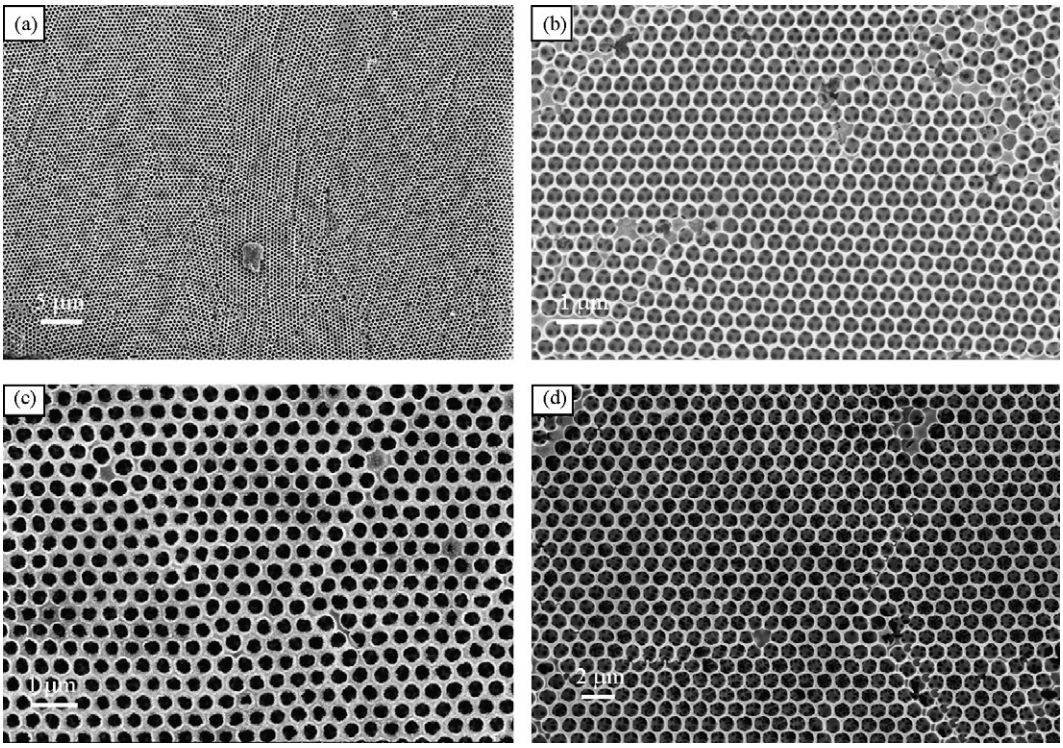

Fig. 4. SEM images of ordered TiO_2 porous materials fabricated with different particle sizes of polystyrene microspheres as templates: (a) low magnification of 480 nm polystyrene, (b) high magnification of 480 nm polystyrene, (c) 600 nm polystyrene, and (d) 1000 nm polystyrene.

same orientation as that of the original polystyrene templates. It is obvious that regular structures can be fabricated using the developed method. A highly ordered hexagonal array was clearly observed for ordered TiO_2 porous films with different pore diameters (480–1000 nm). The hexagonal orientation indicates the cubic close packed (1 1 1) planes oriented parallel to the substrate of glass slides. The air hole formed is due to the removal of polystyrene after calcinations. A triangular pattern below each hole in the first layer can be observed because each sphere rests on three neighboring spheres below. The observation of a regular triangular pattern directly demonstrates the well-ordered three-dimensional porous structure. The spherical template of polystyrene and the periodic opal structure were maintained after calcinations. However, compared with the original template of spherical polystyrene, the pore size after calcinations is smaller because the sol–gel process used in this study causes the walls to shrinkage during calcinations.

3.4. Characterization of ordered TiO_2 porous films

The crystallization of TiO_2 porous films was identified by X-ray diffraction (XRD). Fig. 5 shows the XRD patterns of TiO_2 porous films prepared with different diameters of polystyrene at 550 °C. Peaks centered at 25.47°, 37.91°, 48.21°, and 54.70° (2θ) were clearly observed, which can be assigned as (1 0 1), (0 0 4), (2 0 0), and (2 1 1) orientation of the anatase phase. In addition, a small rutile peak can be observed at 27.44° (2θ), which can be assigned as (1 1 0). The intensity ratio of the characteristic absorption peaks between anatase and rutile was about 4.3 (100:23), 4.7 (100:21) and 13.6 (100:7) when the polystyrene diameters were 480, 600 and 1000 nm, respectively. This result depicts that anatase is the main crystalline phase of TiO_2 at the calcination temperature of 550 °C, and the template diameter used for fabrication of the ordered porous film could influence the crystallization of TiO_2. In addition, the grain sizes of anatase TiO_2, calculated from the Scherrer equation from XRD, were in the range of 7.0–9.7 nm, which is consistent with the results obtained from SEM images. Liu et al. [32] used a photo-assisted sol–gel method to synthesize TiO_2 nanoparticles using titanium isopropoxide as the precursor. The grain sizes of the TiO_2 particles in the absence of the UV-irradiation samples were in the range of 9.8–20.3 nm. Meng et al. [25] assembled a highly order

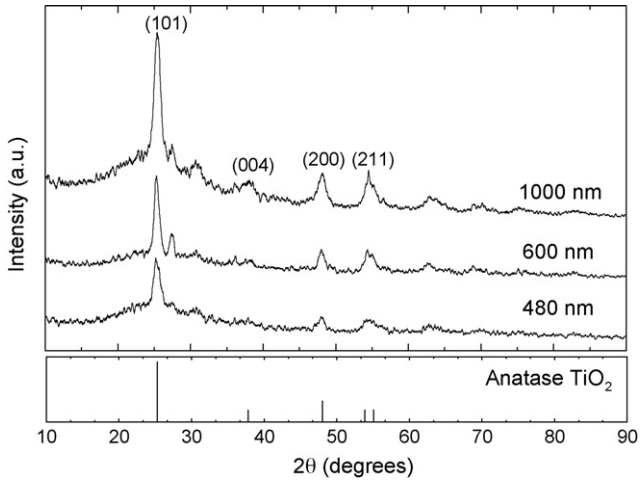

Fig. 5. XRD patterns of ordered TiO_2 porous film calcined at 550 °C.

three-dimensional porous structures with commercial nanosized crystalline TiO_2 particles by a cooperative method in which the fabrication of the template and the infiltration of the voids of the templates was carried out at the same time. The mean size of the TiO_2 particles used was about 13 nm. These results indicate that the grain size of the sol–gel derived TiO_2 nanoparticles prepared in this method is small enough to infill the voids of polystyrene templates. In addition, the particle size of TiO_2 sol can be easily tailored by simply adjusting the pH value of the sol solution, depicting that the combination of sol–gel and template methods is convenient for the fabrication of highly ordered porous materials using the simple one-step technique.

The specific surface area, pore volume and pore size of the ordered TiO_2 porous materials were further examined using N_2 as the adsorbate. Fig. 6 shows the adsorption–desorption isotherms of N_2 at 77 K for the ordered TiO_2 porous films. After the removal of polystyrene calcined at 550 °C, the ordered TiO_2 structure contains mainly anatase. All three different hole sizes of ordered TiO_2 films exhibited similar type IV isotherms with a small amount of high-pressure hysteresis, which indicates the unrestricted monolayer–multilayer adsorption on mesoporous adsorbents. The BET surface areas and pore volumes in TiO_2 sol–gel derived porous films tend to increase when the pore diameters of the ordered structures decreased from 1000 to 480 nm. As depicted in Table 2, the specific surface areas of ordered TiO_2 porous films fabricated with polystyrene of 480, 600, and 1000 nm were 84, 65, and 59 $m^2\ g^{-1}$, respectively. The pore volumes also showed similar tendency and decreased from 0.14 to 0.08 $cm^3\ g^{-1}$ when the particle diameters of polystyrene increased from 480 to 1000 nm. In addition, the BJH pore size distributions for the ordered TiO_2 materials were determined in this study. The average pore diameters were 6.0, 5.5, and 5.1 nm in ordered TiO_2 films fabricated with polystyrene of 480, 600 and 1000 nm, respectively, which is mainly attributed to the mesostructured pore sizes in walls of the macrospheres used for fabricating the opal structure. Yu et al. [15] used surfactant-templated method to synthesize zeolite-like mesoporous TiO_2 nanocrystalline thin films and found that the surface areas and the average pore diameters of the thin films were in the range 40–85 $m^2\ g^{-1}$ and 6.3–8.6 nm, respectively, when the samples were sintered at 500–600 °C. Hirashima et al. [33] prepared the mesoporous TiO_2 xerogel in the presence of different surfactants and found that the specific surface areas and pore volumes of the CTAC-modified xerogel were in the range 34.1–89.3 $m^2\ g^{-1}$ and 0.101–0.312 $cm^3\ g^{-1}$, respectively, which is consistent with the results obtained in this study. This suggests that the developed TiO_2 porous film is a macrostructured mesoporous material and the measured BET surface areas were mostly attributed to the small particle size of the crystallites. In addition, the reproducibility of the single-step fabrication method was examined by performing the BET analysis of three different ordered TiO_2 porous films prepared with 600 nm polystyrene. The average surface area was $67.7 \pm 2.3\ m^2\ g^{-1}$ ($n = 3$), clearly showing that the fabrication of the ordered TiO_2 structure by single-step method is reliable and reproducible.

The highly ordered porous films can be further confirmed by UV–vis spectra. Fig. 7 shows the absorption spectra of TiO_2 films prepared by different diameters of polystyrene. Absorption bands in the range of 300–350 nm were observed. The peak positions of absorbance were at about 304, 313 and 339 nm for ordered TiO_2 porous films prepared with 480, 600, and 1000 nm polystyrene, respectively, indicating that the porous structures are highly ordered over a large area. The absorption edge is found to have a red shift, depicting that the template diameters

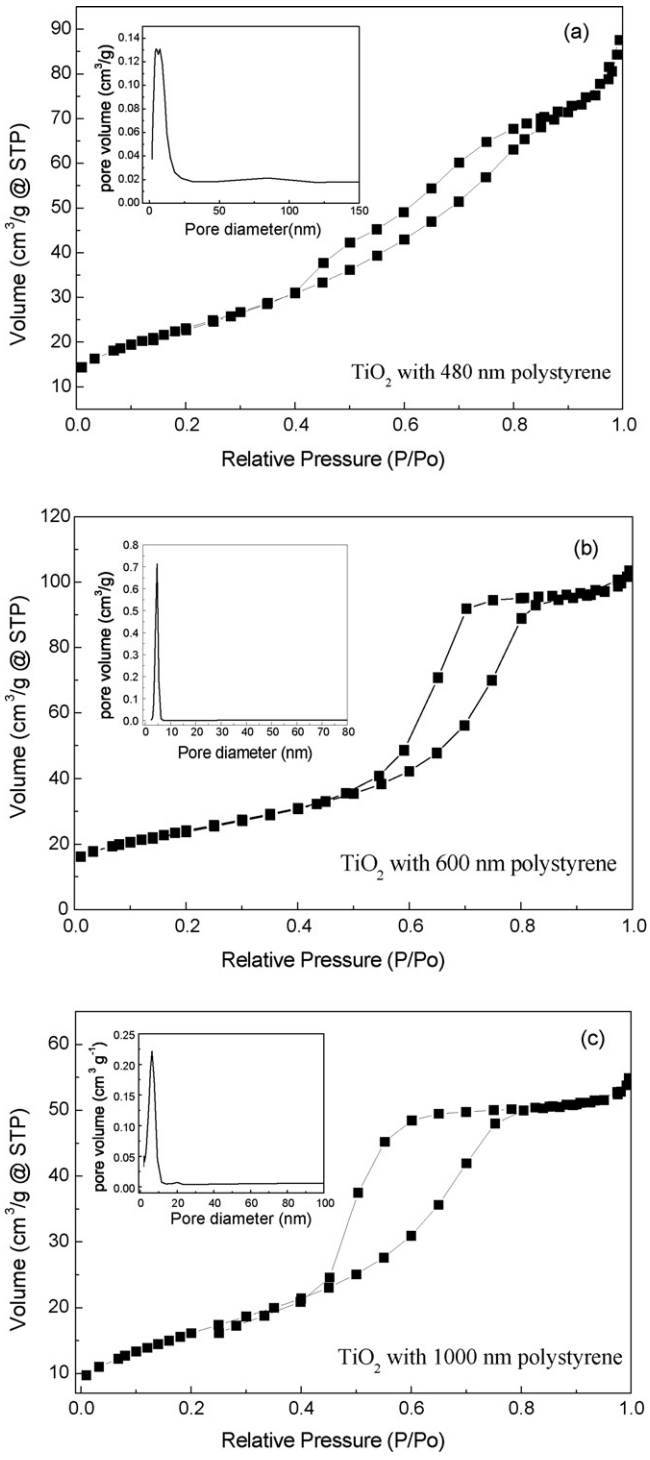

Fig. 6. Nitrogen adsorption–desorption isotherms at 77 K for ordered TiO_2 porous materials using (a) 480 nm, (b) 600 nm, and (c) 1000 nm polystyrene as templates.

Table 2
The surface area, pore volume and pore size of the ordered TiO_2 porous films fabricated with different particle sizes of polystyrene

Polystyrene size (nm)	Specific surface area (S_{BET}) (m^2/g)	Pore volume (cm^3/g)	Adsorption pore size (nm)	Desorption pore size (nm)
480	84	0.14	6.0	5.2
600[a]	67.7 ± 2.3	0.12 ± 0.02	5.9 ± 0.4	4.9 ± 0.4
1000	59	0.08	5.1	3.5

[a] Mean value ± standard deviation ($n = 3$).

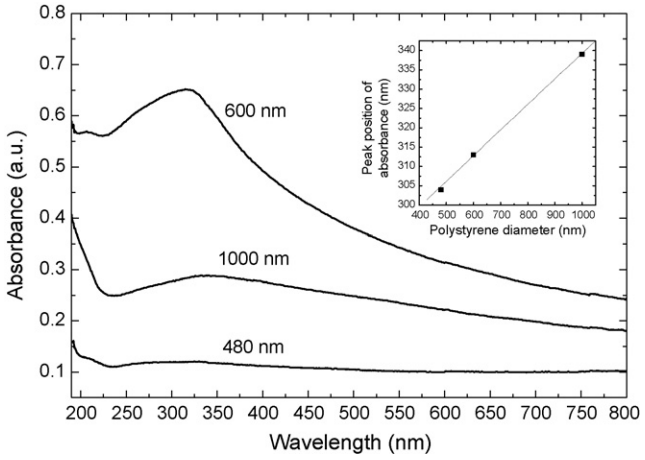

Fig. 7. UV–vis absorption spectra of highly ordered TiO_2 porous materials prepared with polystyrene template with diameters ranging between 480 and 1000 nm.

influence the optical property of ordered TiO_2 porous materials. In addition, a linear relationship between the particle size of template and the peak position to the pore size was obtained. These results demonstrate that highly ordered TiO_2 films with different pore sizes have been successfully fabricated using the method developed in this study.

3.5. Photocatalytic activity

Fig. 8 shows the photocatalytic activity of ordered TiO_2 films toward MB degradation under illumination of UV light at 305 nm. The photodegradation efficiency of MB by porous TiO_2 films increased with the increase in polystyrene diameters from 480 to 1000 nm. In addition, the photodegradation efficiency of MB by porous TiO_2 films was higher than that of Degussa P-25, depicting the high photocatalytic activity of the prepared ordered TiO_2 films.

The photodegradation of MB followed the pseudo-first-order kinetics and the pseudo-first-order rate constant (k_{obs}) for MB degradation increased from 0.0392 min^{-1} for Degussa P-25 to 0.133 min^{-1} for TiO_2 film at 1000 nm. A good linear relationship between rate constant (k_{obs}) and polystyrene diameter was also established. It is noted that the TiO_2 porous film fabricated with 1000 nm has the lowest specific surface area, while the k_{obs} for MB photodegradation is highest. This may probably be attributed to the ease diffusion and the enhanced photoabsorption efficiency of TiO_2 porous film fabricated with large diameter of polystyrene [34,35]. Wang et al. [35] reported that the photocatalytic activity of meso-macroporous TiO_2 in ethylene photodegradation is higher than that of Degussa P-25. The introduction of macroporous channels into mesoporous TiO_2 increased the photocatalytic activity due to the minimization of intradiffusion resistance and the enhancement of photoabsorption efficiency [35]. In the 3-D macroporous–mesoporous materials, the macrochannels can serve as effective paths for light and reactant transportation. This allows the UV light to penetrate more deep inside the hierarchical TiO_2 porous films, resulting in the enhancement of degradation efficiency and rate of MB by TiO_2 photocatalyst fabricated with large diameter of polystyrene.

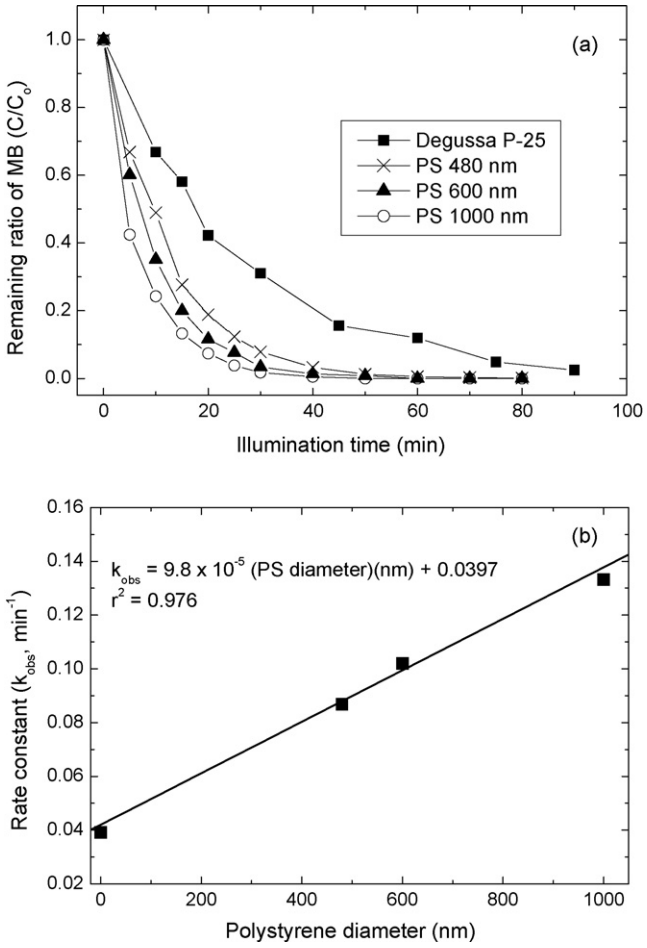

Fig. 8. (a) The photocatalytic degradation of methylene blue and (b) pseudo-first-order rate constants (k_{obs}) as a function of polystyrene diameter under illumination of UV light at 305 nm.

4. Conclusions

In this study, three-dimensional highly ordered TiO_2 porous films with high surface areas were successfully assembled using a simple one-step method in which the fabrication of the tem-

plate and the infiltration of the voids of the templates with TiO_2 sol particles are carried out simultaneously. Polystyrene templates were completely removed at 424 °C and the phase transformation of TiO_2 from amorphous to crystalline anatase occurred at 360 °C. The structural studies show that the ordered TiO_2 porous materials remain mainly anatase after annealing at 550 °C. The highly ordered porous structures fabricated with the above approach appear to have high specific surface area from the internal pores of the framework rather than the pore sizes of template before calcinations. The UV–vis spectra show a red-shift upon increasing the particle size of polystyrene and a linear relationship between the particle size of template and the peak position of absorbance was obtained. In addition, the photodegradation efficiency of MB by TiO_2 porous films increased with the increase in polystyrene diameters ranging from 480 to 1000 nm. The pseudo-first-order rate constants (k_{obs}) for MB degradation were in the range 0.087–0.133 min^{-1}, which is higher than that of Degussa P-25 (0.0392 min^{-1}). These results illustrate the potential of the hierarchical TiO_2 porous films as an effective material which can be widely applied in the field of photocatalysis to purify water and wastewater.

Acknowledgement

The authors thank National Science Council, Taiwan for financial support under grant No. NSC 95-2113-M-007-008.

References

[1] F.Z. Huang, M.F. Zhou, Y.B. Cheng, R.A. Caruso, Al-containing porous titanium dioxide networks: sol–gel synthesis within agarose gel template and photocatalytic activity, Chem. Mater. 18 (2006) 5835–5839.
[2] Z.-Z. Gu, R. Horie, S. Kubo, Y. Yamada, A. Fujishima, O. Sato, Fabrication of a metal-coated three-dimensionally ordered macroporous film and its application as a refractive index sensor, Angew. Chem. Int. Ed. 41 (2002) 1153–1156.
[3] D. Chatterjee, S. Dasgupta, Visible ligh induced photocatalytic degradation of organic compounds, J. Photochem. Phobiol. C: Photochem. Rev. 6 (2005) 186–205.
[4] R.A. Doong, C.H. Chen, R.A. Maithreepala, S.M. Chang, The influence of pH and cadmium sulfide on the photocatalytic degradation of 2-chlorophenol in titanium dioxide suspensions, Water Res. 35 (2001) 2873–2880.
[5] C.C. Chen, P.X. Lei, H.W. Ji, W.H. Ma, J.C. Zhao, H. Hindaka, N. Serpone, Photocatalysis by titanium dioxide and polyoxometalate/TiO_2 cocatalysts. Intermediates and mechanistic study, Environ. Sci. Technol. 38 (2004) 329–337.
[6] M.A. Barakat, Y.T. Chen, C.P. Huang, Removal of toxic cyanide and Cu(II) Ions from water by illuminated TiO_2 catalyst, Appl. Catal. B: Environ. 53 (2004) 13–20.
[7] C.C. Su, K.F. Lin, Y.H. Lin, B.H. You, Preparation and characterization of high-surface-area titanium dioxide by sol–gel process, J. Porous Mater. 13 (2006) 251–258.
[8] C.H. Ao, S.C. Lee, Combination effect of activated carbon with TiO_2 for the photodegradation of binary pollutants at typical indoor air level, J. Photochem. Photobiol. A: Chem. 161 (2004) 131–140.
[9] J.C. Lee, M.S. Kim, B.W. Kim, Removal of paraquat dissolved in a photoreactor with TiO_2 immobilized on the glass-tubes of UV lamps, Water Res. 36 (2002) 1776–1782.
[10] X.W. Zhang, M.H. Zhou, L.C. Lei, Preparation of anatase TiO_2 supported on alumina by different metal organic chemical vapor deposition methods, Appl. Catal. A: Gen. 282 (2005) 285–293.
[11] F. Bosc, P. Lacroix-Desmazes, A. Ayral, TiO_2 anatase-based membrane with hierarchical porosity and photocatalytic properties, J. Colloid Interface Sci. 304 (2006) 545–548.
[12] O.D. Velev, P.M. Tessier, A.M. Lenhoff, E.W. Kaler, Materials—A class of porous metallic nanostructures, Nature 401 (1999) 548.
[13] W. Ho, J.C. Yu, S.C. Lee, Synthesis of hierarchical nanoporous F-doped TiO_2 sphere with visible light photocatalytic activity, Chem. Commun. (2006) 1115–1117.
[14] L. Zhao, Y. Yu, L. Song, M. Ruan, X. Hu, A. Larbort, Preparation of mesoporous titania film using nonionic triblock copolymer as surfactant template, Appl. Catal. A: Gen. 263 (2004) 171–177.
[15] J.C. Yu, X.C. Wang, X.Z. Fu, Pore-wall chemistry and photocatalytic activity of mesoporous titania molecular sieve films, Chem. Mater. 16 (2004) 1523–1530.
[16] Y. Xia, R. Gates, Y. Yin, Y. Lu, Monodispersed colloidal spheres: old materials with new applications, Adv. Mater. 12 (2000) 693–713.
[17] P. Yang, A.H. Rizvi, B. Messer, B.F. Chmelka, G.M. Whitesides, G.D. Stucky, Patterning porous oxides within microchannel networks, Adv. Mater. 13 (2001) 427–431.
[18] Y. Xia, G.M. Whitesides, Soft lithography, Annu. Rev. Mater. Sci. 28 (1998) 153–184.
[19] A.A. Zakhidov, I.I. Khayrullin, R.H. Baughman, Z. Iqbat, CVD synthesis of carbon-based metallic photonic crystals, Nanostruct. Mater. 12 (1999) 1089–1095.
[20] O.D. Velve, E.W. Kaler, Structured porous materials via colloidal crystal templating: from inorganic oxides to metals, Adv. Mater. 12 (2000) 531–534.
[21] P.T. Hammond, Form and function in multilayer assembly: new applications at the nanoscale, Adv. Mater. 16 (2004) 1271–1293.
[22] A. Stein, Advances in microporous and mesoporous solids—highlights of recent progress, Adv. Mater. 15 (2003) 763–775.
[23] A. Stei, R.C. Schroden, Colloidal crystal templating of three-dimensionally ordered macroporous solids: materials for photonics and beyond, Curr. Opin. Solid State Mater. Sci. 5 (2001) 553–564.
[24] P. Ni, P. Dong, B. Cheng, X. Li, D. Zhang, Synthetic SiO_2 opals, Adv. Mater. 13 (2001) 437–441.
[25] Q.-B. Meng, C.-H. Fu, Y. Einaga, Z.-Z. Gu, A. Fujishima, O. Sato, Assembly of highly ordered three-dimensional porous structure with nanocrystalline TiO_2 semiconductors, Chem. Mater. 14 (2002) 83–88.
[26] S.M. Chang, R.A. Doong, Chemical-composition-dependent metastability of tetragonal ZrO_2 in sol–gel-derived films under different calcination conditions, Chem. Mater. 17 (2005) 4837–4844.
[27] S.M. Chang, R.A. Doong, The effect of chemical states of dopants on the microstructures and band gaps of metal-doped ZrO_2 thin films at different temperatures, J. Phys. Chem. B 108 (2004) 18098–18103.
[28] H.C. Tsai, R.A. Doong, Simultaneous determination of renal clinical analytes in serum using hydrolase- and oxidase-encapsulated optical array biosensors, Anal. Biochem. 334 (2004) 183–192.
[29] S.M. Chang, R.A. Doong, Characterization of Zr-doped TiO_2 nanocrystals prepared by a non-hydrolytic sol–gel method at high temperatures, J. Phys. Chem. B 110 (2006) 20808–20814.
[30] C.A. LeDuc, J.M. Campbell, J.A. Rossin, Effect of lanthana as a stabilizing agent in titanium dioxide support, Ind. Eng. Chem. Res. 35 (1996) 2473–2476.
[31] B. Zhang, C. Chen, K. Shi, S. He, X. Liu, Z. Du, K. Yang, Preparation and characterization of nanocrystal grain TiO_2 porous microspheres, Appl. Catal. B 40 (2003) 253–258.
[32] H. Liu, W. Yang, Y. Ma, Y. Cao, J. Yao, J. Zhang, T. Hu, Synthesis and characterization of titania prepared by using a photoassisted sol–gel method, Langmuir 19 (2003) 3001–3005.
[33] H. Hirashima, H. Imai, V. Balek, Preparation of meso-porous TiO_2 gels and their characterization, J. Non-Cryst. Solids 285 (2001) 96–100.
[34] Z.Y. Yuan, B.L. Su, Insights into hierarchically meso-macroporous structured materials, J. Mater. Chem. 16 (2006) 663–677.
[35] X.C. Wang, J.C. Yu, C.M. Ho, Y.D. Hou, X.Z. Fu, Photocatalytic activity of a hierarchically macro/mesoporous titanium, Langmuir 21 (2005) 2552–2559.